A Study on the Mechanics of Shear Spinning of Cones

Jae Hun Kim
ERC/NSDM, at Pusan National University,
Jangjun-dong, Kumjeong-ku, Buasn 609-735, Korea
Jun Hong Park
CANSMC, at Dong-A University,
Hadan2-dong, Saha-gu, Busan 604-714, Korea
Chul Kim*
Research Institute of Mechanical Technology, at Pusan National University,
Jangjun-dong, Kumjeong-ku, Buasn 609-735, Korea

The shear spinning process, where the plastic deformation zone is localized in a very small portion of the workpiece, shows a promise for increasingly broader application to the production of axially symmetric parts. In this paper, the three components of working force are calculated by the newly proposed deformation model in which the spinning process is understood as shearing deformation after uniaxial yielding by bending, and shear stress, τ_{rz} becomes k, yield limit in pure shear, in the deformation zone. The tangential forces are first calculated and the feed forces and the normal forces are obtained by the assumption of uniform distribution of roller pressure on the contact surface. The optimum contact area is obtained by minimizing the bending energy required to get the assumed deformation of the blank. The calculated forces are compared with experimental results. A comparison shows that theoretical prediction is reasonably in good agreement with experimental results.

Key Words: Bending Energy, Optimum Contact Area, Shear Spinning, Tangential Force

Nomenclature

E : Young's modulus Kg/mm^2
f : Feed of roller
F_t : Tangential force component in shear spinning
F_f : Feed force component
F_n : Normal force component
G : Modulus of rigidity, Kg/mm^2
k : Yield limit in shear, Kg/mm^2
M_{EP} : Bending moment, respectively, required to bring about yielding of one half portion of a rectangular section element
N : Speed of rotation of mandrel
m : Contact factor
r_0 : Corner radius of roller
r_a, r_c, r_i, r_b : Cone radii
S : Area BQFCRB
S_1 : Area BMICRB
S_2 : Area BQFIMB
t_0 : Initial thickness of blank
t_f : Final thickness of cone
$\dot{w}$: Total energy of deformation
z_D : z-value of the curve SMR
α, ALPA : Half cone angle of mandrel
$\bar{\sigma}_m$, MES : Mean effective stress
$\int d\bar{\varepsilon}$: Total effective strain
$\dot{\varepsilon}$: Strain rate
$\dot{\varepsilon}_{rz}, \dot{\varepsilon}_{\theta z}, \dot{\varepsilon}_{r\theta}$: Strain rate tensors in cylindrical coordinates
$\bar{\varepsilon}$, FES : Finite effective strain
$\bar{\varepsilon}_m$: Mean effective strain in the deformation zone

* Corresponding Author,
E-mail : chulki@pusan.ac.kr
TEL : +82-51-510-2489; **FAX** : +82-51-512-9835
Research Institute of Mechanical Technology, at Pusan National University, Jangjun-dong, Kumjeong-ku, Buasn 609-735, Korea. (Manuscript **Received** November 1, 2005; **Revised** March 7, 2006)

η : Length of blank in its rotational direction
η_m : Assumed actual contact length
η_p : Ideal geometric contact length
$\bar{\rho}, \bar{\rho}'$: Radii of curvature of deformation

1. Introduction

The aim of this study is to help better understating of the process of shear spinning and to propose a better method for prediction of the power required. The prediction of the power required to deform the blank is very important in the choice for the proper equipment and the process variables of the specified job. Furthermore, this power is the predominant factor affecting to the interactional force between the roller and the cone.

So a number of investigations on the spinning process, both theoretical and experimental, have reported in the previous literatures. For example, Colding (1959) considered cone spinning as a combination of rolling and extrusion process, whereas Kalpackcioglu (1961) assumed a simple shear mechanism for the analysis of the working forces. The complex straining effect was introduced into the solution of cone spinning by Avitzur and Yang (1960), Kobayashi et al.(1961), and Hayama et al.(1964) But their equations for predicting the tangential component force are of a complex nature and require the long computation time for its solution. Hayama and Amano (1975) studied the form of contact between blank and roller during shear spinning by experimental and theoretical procedure. Moreover Hayama (1975) estimated concretely the three components of working force using the contact area between blank and roller obtained from his previous work. A test method for determining the spinability of cones was proposed by Kegg (1961). This consists of shear spinning a blank on an ellipsoidal mandrel. On the other hand, Kalpakcioglu proposed the stress system to get the maximum allowable reduction in shear spinning process. Sortais et al.(1963) studied the cone wall thickness variation in conventional spinning of cones and derived the theoretical tangential force component by the deformation energy method. However each previous theory for the working forces agreed with the experimental data for only a limited range of process variables, and did not give good results for other working conditions.

In this paper, for the reasonable derivation of tangential force F_t, the new deformation model was assumed to minimize the redundant work over $\dot{W}_{rz}$ and to keep the constant radial position during the deformation. The form of contact area obtained from the experiments of Hayama and Amano (1975) was utilized to get the contact factor, m by the concept of uniform distribution of pressure on the roller that was originally proposed by Kobayashi et al.

After calculating the tangential force F_t, the other components of the working forces, the feed force F_f and normal force F_n, were computed by using the above assumptions. And the calculated working forces were compared with the experimental results.

2. Mechanics of Shear Spinning of Cones

2.1 Deformation mode

The deformation mechanism of shear spinning of cones is shown schematically in Fig. 1(a). The blank material is a disk of diameter, D_b and uniform thickness, t_o. The disk is mounted on a circular conical mandrel, which is clamped to the head of the spinning machine, and rotated. A forming roller is driven on tracks on the bed of the machine parallel to the side of the mandrel. The process is characterized by the fact that the radial position of an element in the blank remains constant during deformation and the angular velocity is constant through the whole work piece except the deformation zone. This demands that the initial disk thickness, t_o and the final thickness of the cone, t_f for the half cone angle α are related by the equation.

$$t_f = t_o \sin \alpha \tag{1}$$

And, for simplicity, it is assumed that during one revolution of the mandrel, the roller holds the same position, and after one complete revolution of the mandrel, the roller feeds $f \sin \alpha$ to x-direction and $f \cos \alpha$ to z-direction in Fig. 1(a).

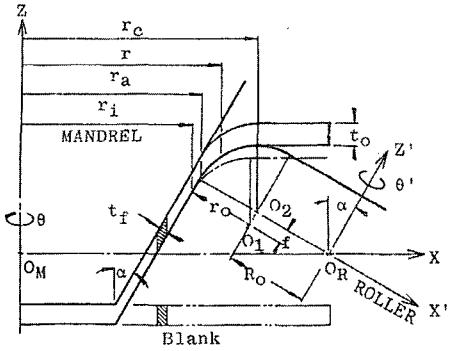

(a) R-Z plane

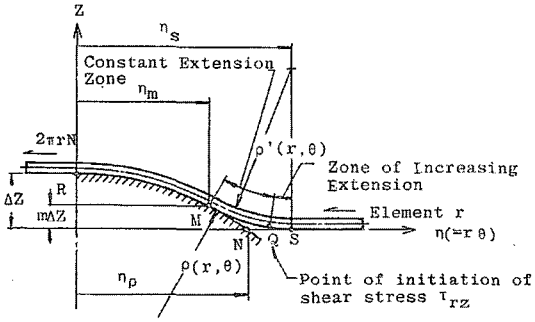

(b) Z-η plane

Fig. 1 Schematic description of the deformation in shear spinning of cones

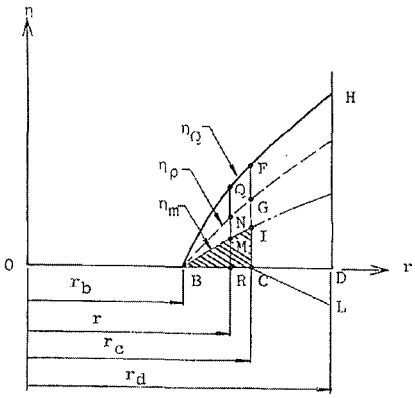

(a) Deformation region in -r plane

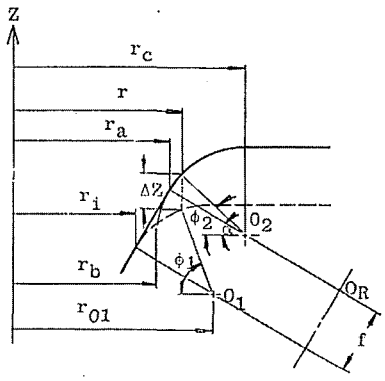

(b) Shear deformation

Fig. 2 Model of deformation

The form of deformation of the z-η plane about a radial element of the blank is assumed to take the form of the solid line SQMR in Fig. 1 (b), where z and η indicate respectively the height and the length of the blank in its rotational direction.

Figure 1(b) corresponds to Fig. 2(a). The curved line, η_m shows where the roller begins to make contact with the blank, while the line, η_ρ is the one obtained as a result of the geometrical calculation. The line where the bending starts can be drawn as BQFH in Fig. 2(a) and the shaded area, BIC, is the actual contact area. Fig. 2(b) shows the radial region of deformation. The deformation region is bounded by r_b and r_c.

Let us consider an element, r in Fig. 1(b). The element starts to deform at point S where its radius of curvature ρ' is tend to infinity. After passing point S, the radius of curvature decreases gradually and at point Q one-half portion of an element becomes to yield by uniaxial tension or compression by bending.

After passing the point Q, the circumferential extension of an element r is assumed to be constant until it reaches the point M while the shear strain, γ_{rz} is increased monotonically from zero to $\left(\frac{\theta_Q-\theta_m}{\theta_Q}\right)(\cot\phi_2-\cot\phi_1)$ along QM, where θ_Q and θ_M are given by Eq. (12). The difference of $\left(\frac{\partial\gamma_{rz}}{\partial r}dr\right)$ makes the radius of curvature of the element decrease along QM and the element reaches the point M.

After passing the point M, the extension of an element changes its sign and assumed to be constant while shear strain, γ_{rz} is increased monotonically, starting from $\left(\frac{\theta_Q-\theta_m}{\theta_Q}\right)(\cot\phi_2-\cot\phi_1)$ to $(\cot\phi_1)$ on the roller along MR.

After reaching the point R, the circumferential extension of an element, r will be unloaded elastically.

In Fig. 2(a), the plastic deformation occurs

only in region BFCB and elastic bending occurs in region FHLCF.

To get the contact length, η_m, we assumed the following relations

$$\bar{\rho}(r)=\frac{\eta_m^2}{2(1-m)\Delta z}=\frac{\eta_\rho^2}{2\Delta z} \tag{2}$$

and

$$\bar{\rho}'(r)=\frac{m}{1-m}\bar{\rho}(r) \tag{3}$$

Noting that the ideal geometric contact length, η_ρ is given by

$$\eta_\rho=r\theta_0 \tag{4}$$

where $\bar{\rho}(r)$ and $\bar{\rho}'(r)$ are the mean radius of curvature for $\rho(r,\theta)$ and $\rho'(r,\theta)$ respectively and θ_0 is the ideal geometric contact angle and is given by Eq. (13).

From Eq. (2), we obtain

$$\eta_m=\sqrt{1-m}\cdot\eta_\rho \tag{5}$$

The radius of curvature at Point Q of an element r is given by ρ_{EP}

$$\rho_Q'=\rho_{EP}=\frac{Et_o}{4\sqrt{3}\,k} \tag{6}$$

$$M_Q'=M_{EP}=\frac{11t_o^2k}{16\sqrt{3}} \tag{7}$$

According to the foregoing deformation mechanism, we obtain the following geometrical relations from Figs. 1 and 2.

$$r_c=r_a+r_o\cdot\cos\alpha \tag{8}$$

$$r_i=r_a-f\cdot\sin\alpha \tag{9}$$

$$r_b=r_a-0.5\cdot f\cdot\sin\alpha+\left(r_o-\sqrt{r_o^2-\frac{f^2}{4}}\right)\cos\alpha \tag{10}$$

$$f_{o1}=r_c-f\cdot\sin\alpha \tag{11}$$

$$\theta_m=\eta_m/r,\quad \theta_Q=\eta_Q/r \tag{12}$$

$$\theta_0=\cos^{-1}\left\{\frac{1}{r}\left(r_c-\frac{-D+\sqrt{D^2-CF}}{C}\right)\right\} \tag{13}$$

where,

$A=2(r_c+R_0\cos\alpha)$

$B=r^2+(z-z_{02})^2+2(z-z_{02})R_0\sin\alpha-r_c^2-r_0^2$

$C=A^2+4R_0^2\cdot\sin^2\alpha$

$D=AB-2R_0^2(z-z_{02})\sin 2\alpha$

$F=B^2-4R_0^2\{r_0^2-(z-z_{0z})^2\cos^2\alpha\}$

$$z-z_{02}=\sqrt{r_0^2-(r_{01}-r)^2}-f\cos\alpha \quad \text{for } r_b\le r\le r_{01}$$
$$=r_0-f\cos\alpha \quad \text{for } r_{01}\le r\le r_c$$

$$\Delta z=f\cos\alpha+(r_c-r)\tan\phi_2-(r_{01}-r)\tan\phi_1 \quad \text{for } r_b\le r\le r_{01} \tag{14}$$
$$=f\cos\alpha+(r_c-r)\tan\phi_2-r_o \quad \text{for } r_{01}\le r\le r_c$$

$$\cot\phi_1=\frac{r_{01}-r}{\sqrt{r_o^2-(r_{01}-r)^2}} \quad \text{for } r_b\le r\le r_{01} \tag{15a}$$
$$=0 \quad \text{for } r_{01}\le r\le r_c$$

$$\cot\phi_2=\frac{r_c-r}{\sqrt{r_o^2-(r_c-c)^2}} \quad \text{for } r_b\le r\le r_c \tag{15b}$$

2.2 Strain rates and stresses

For the calculation of strain rates and stresses induced from foregoing deformation mode shown in Fig. 1(b), it is assumed that the point Q is very near from point S and not only the outermost fiber but also the neutral fiber of point Q is elongated by the constant tangential strain, ε_θ given by

$$\varepsilon_\theta=k/\sqrt{3}\cdot G \tag{16}$$

which is required to get yielding the material in uniaxial tension or compression, where the constant k is the yield limit in pure shear.

This tangential strain, ε_θ is kept constant during second phase of straining by γ_{rz}.

For brevity, it is assumed that the material is incompressible in the elastic as well as the plastic range. The circumferential extension, ε_θ would therefore be accompanied by the lateral contraction given by

$$\varepsilon_r=\varepsilon_z=-\varepsilon_\theta/2 \tag{17}$$

which satisfies the condition of incompressibility in the elastic as well as the plastic range, and is valid under the condition of Eq. (20). After passing the point Q in Fig. 1(b), the circumferential extension of an element r is assumed to be constant until it reaches the point M while the shear strain, γ_{rz} is increased monotonically from zero to $\frac{\theta_Q-\theta}{\theta_Q}(\cot\phi_2-\cot\phi_1)$ along QM. After passing M, the extension of an element changes its sign and assumed to be constant while shear strain, γ_{rz} is increased monotonically, starting from $\frac{\theta_Q-\theta_m}{\theta_Q}(\cot\phi_2-\cot\phi_1)$ to $\frac{\theta_Q-\theta}{\theta_Q}(\cot\phi_2-\cot\phi_1)$ on the

roller along MR.

After reaching the point R, the circumferential extension and shear strain will be unloaded elastically.

During second phase straining, we have the shear strain, γ_{rz} given by

$$\gamma_{rz}=\frac{\theta_Q-\theta}{\theta_Q}(\cot\phi_2-\cot\phi_1) \tag{18}$$

which is based on the assumption of the deformation mode, and all the others of ε_{ij} become zero, that is,

$$\gamma_{\theta z}=\gamma_{r\theta}=0 \tag{19}$$

Moreover, within the frame work of beam theory, we assume that

$$\sigma_r=\sigma_z=0 \text{ and } \tau_{r\theta}=\tau_{\theta z}=0 \tag{20}$$

These are based on the assumption that the element r is an independent beam of width dr to which the bending moment, M_{EP} and shear stress, γ_{rz} are only applied.

Then, the only non-vanishing stress components are

$$\sigma_\vartheta=\sigma_\vartheta(r,\ \theta),\ \tau_{rz}=\tau_{rz}(r,\ \theta) \tag{21}$$

The non-vanishing components of deviatoric stress are then given by

$$\sigma_r'=\sigma_z'=\frac{\sigma_\theta}{3},\ \sigma_\theta'=\frac{2}{3}\sigma_\theta \tag{22}$$

The rate at which the stresses do work in deforming a continuous medium is given by

$$\dot{W}=\sigma_\theta\dot{\varepsilon}_\theta+\tau_{rz}\dot{\tau}_{rz} \tag{23}$$

Finally, the stress-strain relations of Prandtl-Reuss material require that

$$\dot{\sigma}_\vartheta=3G\left(\dot{\varepsilon}_\theta-\frac{\dot{W}}{3k^2}\sigma_\theta\right)$$

and (24)

$$\dot{\tau}_{rz}=G\left(\dot{\gamma}_{rz}-\frac{\dot{W}}{k^2}\tau_{rz}\right)$$

in the plastic range BFCB of Fig. 2.

From Eq. (18), $\dot{\gamma}_{rz}$ is the mean shear strain rate and is given by

$$\dot{\gamma}_{rz}=(\cot\phi_2-\cot\phi_1)/\Delta t$$

where (25)

$$\Delta t=\frac{\eta_Q}{2\pi Nr}$$

For the integration of these equations, let us suppose that the element r is first pulled by $\sigma_\theta=\sqrt{3}\,k$ until it reaches the yield limit in tension at point Q, and then sheared while the extension is kept constant.

For this second straining phase Eq. (23) apply with $\dot{\varepsilon}_\theta=0$ and hence,

$$\dot{W}=\dot{\tau}_{rz}\dot{\gamma}_{rz} \tag{26}$$

Thus, we now must integrate the equation,

$$\dot{\sigma}_\theta=-\frac{G}{k^2}\sigma_\theta\tau_{rz}\dot{\gamma}_{rz}$$

and (27)

$$\dot{\tau}_{rz}=G\frac{(k^2-\tau_{rz}^2)}{k^2}\dot{\gamma}_{rz}$$

under the initial conditions

$$\sigma_\theta=\sqrt{3}\,k,\ \tau_{rz}=0 \text{ for } \theta=\theta_Q \tag{28}$$

where

$$(\gamma_{rz})_{\theta=\vartheta_0}=0 \tag{29}$$

Moreover, the Mises' yield condition requires that, for any r and θ in the region BFCB.

$$\left(\frac{\sigma_\theta}{\sqrt{3}}\right)^2+\tau_{rz}^2+\tau_{rz}^2=k^2 \tag{30}$$

throughout this second straining phase.

Integrating Eq. (27) and taking account of Eq. (28), we obtain

$$\tau_{rz}(r,\ \theta)=k\tanh\left\{\frac{G}{k}\gamma_{rz}(r,\ \theta)\right\} \tag{31}$$

$$\sigma_\vartheta(r,\ \theta)=\sqrt{3}\,k\sec h\left\{\frac{G}{k}\gamma_{rz}(r,\ \theta)\right\} \tag{32}$$

For the Mises' material, we have

$$\tau_{rz}(r,\ \theta)=k\quad \sigma_\vartheta(r,\ \theta)=\theta \text{ for } G\to\infty \tag{33}$$

It is easily verified that Eqs. (31) and (32) satisfy Eq. (27). Eq. (26) can be rewritten by utilizing Eq. (33) for the Mises material

$$\dot{W}=k\dot{\gamma}_{rz} \text{ for region BFCB} \tag{26}'$$

The first relation of Eq. (33) was first utilized

to explain the shear spinnability of metals. The results of experiments for spinnability of ductile metals were in good agreements with theoretical predictions based on this assumption.

2.3 Forming power

The instantaneous rate of deformation energy, $d\dot{W}_{rz}$ due to shear strain rate, $\dot{\gamma}_{rz}$ in the region BFCB in Fig. 2(a), become

$$\begin{aligned} d\dot{W}_{rz} &= \int_{\theta} k\dot{\gamma}_{rz} t_o dr r d\theta \\ &= 2\pi r N k t_o (\cot\phi_2 - \cot\phi_1)\, dr \end{aligned} \tag{34}$$

On the line BQF and BMI, we obtain the rate of bending energy, $d\dot{W}_B$ due to bending moment, M_{EP} as follows

$$d\dot{W}_B = 2\frac{M_{EP}}{\rho_{EP}} 2\pi r N dr = 2\pi r N \left(\frac{22 t_o k^2}{4E}\right) dr \tag{35}$$

The external work input is closely approximated by

$$d\dot{W}_E = 2\pi r N dF_t \tag{36}$$

where dF_t is an instantaneous tangential force component on the roller along $\theta_m dr$.

By equating the energy consumed to the external work input, we obtain the following relation.

$$d\dot{W}_E = d\dot{W}_{rz} + d\dot{W}_B \tag{37}$$

Inserting Eqs. (34) ~ (36) into Eq. (37), we obtain the instantaneous tangential force,

$$\begin{aligned} F_t &= \int_{r_b}^{r_c} \left\{ k t_o (\cot\phi_2 - \cot\phi_1) + \frac{22 k^2 t_o}{4E} \right\} dr \\ &= k t_o \left(\sqrt{r_o^2 - (r_b - r_{01})^2} - \sqrt{r_o^2 - (r_b - r_{01})^2} \right) \\ &\quad + \frac{2 k^2 t_o}{4E} (r_c - r_b) \end{aligned} \tag{39}$$

where

$$r_c - r_b = \frac{f}{2}\sin\alpha + \sqrt{r_o^2 - \frac{f^2}{4}}\cos\alpha$$

$$r_b - r_{01} = \frac{f}{2}\sin\alpha - \sqrt{r_o^2 - \frac{f^2}{4}}\cos\alpha$$

For the perfectly plastic-elastic material, k is given by $\sigma_y/\sqrt{3}$ where σ_y is the yield limit in simple tension, and for the strain-hardening material, k is given by $\bar{\sigma}/\sqrt{3}$ where $\bar{\sigma}$ is the instantaneous effective flow stress in simple tension.

To compute the Eq. (39), k is assumed to be constant and is given by $\bar{\sigma}_m/\sqrt{3}$ where $\bar{\sigma}_m$ is the effective stress for the mean effective strain, $\bar{\varepsilon}_m$, in the deformation. And the mean effective strain can be obtained as follows

$$\begin{aligned} \bar{\varepsilon}_m &= \frac{1}{r_c - r_b} \int_{r_b}^{r_c} \frac{\cot\phi_2}{\sqrt{3}} dr \\ &= \frac{\sqrt{r_o^2 - (r_c - r_b)^2}}{\sqrt{3}(r_c - r_b)} \end{aligned} \tag{40}$$

This definition for $\bar{\sigma}_m$ is the average value of $\bar{\sigma}$ in the deformation zone, and is different from that given by Kobayashi et al.,(1961).

They defined the mean effective stress $\bar{\sigma}_m$ as

$$\bar{\sigma}_m = \int \bar{\sigma} d\bar{\varepsilon} \Big/ \int d\bar{\varepsilon} \tag{41}$$

It is evident from Eq. (39) that the evaluation of F_t for given material requires knowledge of the stress-strain curve at the shear spinning deformation rates.

These strain rates can be estimated from the second straining of γ_{rz} and bending strain from the equation,

$$\dot{\bar{\varepsilon}} = \frac{\dot{\bar{\gamma}}}{\sqrt{3}} = 2\pi r N \left(\cot\phi_2 - \cot\phi_1 + \frac{22k}{4E}\right) \Big/ \eta_Q \sqrt{3} \tag{42}$$

where η_Q is given by Eqs. (2) and (3).

$$\eta_Q = \eta_o / \sqrt{1 - m(r)} \tag{43}$$

For the average value of the effective strain rates, the value $\dot{\bar{\varepsilon}}$ for $r = (r_c + r_b)/2$ was taken, and is given by

$$\dot{\bar{\varepsilon}}_{avg} = 2\pi r N \left(\cot\phi_2 - \cot\phi_1 + \frac{22k}{4E}\right) \Big/ \eta_Q \sqrt{3} \Big|_{r=(r_c+r_b)/2} \tag{44}$$

in which, to compute η_Q, $m(r)$ was suggested to have a value shown in the next section.

2.4 Forming force component

The two force components, F_r and F_z, too, are important from the point of view of machine design in spinning. These components are shown in the force diagram of Fig. 3.

If it is assumed that a normal stress P acting on the contact surface between the roller and cone is uniformly distributed, then we obtain F_r and F_z as a function of F_t.

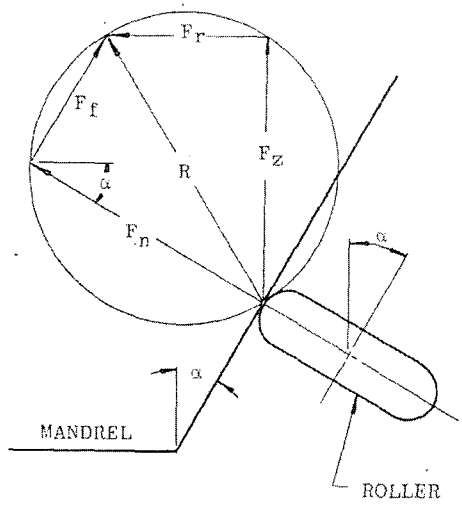

Fig. 3 Force system

$$F_r=\frac{F_t}{A_t}A_r=PA_r \text{ and } F_z=\frac{F_t}{A_t}A_z=PA_z \quad (45)$$

The effect of friction on the contact surface in Eq. (45) is neglected and A_t, A_r and A_z are the projected areas of the contact surface in the tangential, radial, and axial direction respectively.

As soon as the ratios of projected area of the contact surfaces are known, the two force component, F_r and F_z, can be obtained from Eq. (45) using the tangential force component, F_t, determined from Eq. (39).

The projected contact areas for the tangential, radial, and axial direction are given by

$$A_t=\int_{r_b}^{r_c}\Delta z(1-m)\,dr \quad (46)$$

$$A_t=\int_{r_b}^{r_c}\sqrt{(1-m)}\,\eta_\rho \cot\phi_2 dr \quad (47)$$

$$A_t=\int_{r_b}^{r_c}\sqrt{(1-m)}\,\eta_\rho dr \quad (48)$$

where it is necessary to get the value of m for computing the area A_t, A_r and A_z. The form of contact between blank and roller during shear spinning is originally investigated by experimental procedure.

Hence, in this paper, it is suggested that m is a function of r as

$$m(r)=m_c\frac{r-r_b}{r_c-r_b} \quad (49)$$

where m_c has to be determined so as to fit the theoretical forces to the experimental values.

The author, therefore, tried to decide the optimum value of m_c by minimizing the total energy of bending consumed in the model of deformation. The model of deformation is shown in Figs. 1 and 2. The curved line, η_m shows that the roller begins to make contact with the blank, while the line, η_ρ is obtained by the geometrical relations.

If the form of deformation in the $\eta-z$ plane about a radial element of the blank is assumed to take the form of the solid line SQMR in Fig. 1, the line where bending starts can be drawn as BQF (η_Q line) in Fig. 2.

Appling Eq. (2) and Eq. (43) to Eq. (3), then

$$\frac{\eta_m}{\bar\rho}=\frac{\eta_Q-\eta_m}{\bar\rho'} \quad (50)$$

As the form of contact of the shaded section, BIC, varies depending on the position of the point I, the optimum form of contact will be obtained by minimizing the total bending energy calculated on the model of deformation.

The bending energy on the shaded portion, BIC, can be calculated by the following equation.

$$\iint_F M_P\frac{1}{\rho}dr d\eta=\int_r M_P\frac{1}{\bar\rho}\eta_m dr \quad (51)$$

while the bending energy on the section, BFG, may be also written as

$$\iint_F M_P\frac{1}{\rho'}dr d\eta=\int_r M_P\frac{1}{\bar\rho'}(\eta_Q-\eta_m)\,dr \quad (52)$$

where M_P means the fully plastic bending moment per unit width of the blank, and will be the value $(t_o^2\bar\sigma_m/4)$.

The total bending energy can be obtained from adding Eq. (51) to Eq. (52), and inserting Eq. (50)

Then

$$W_B=\int_r 2M_P\frac{\eta_m}{\bar\rho}dr=2M_P\int_r\frac{2\Delta z}{\eta_\rho}\sqrt{1-m(r)}\,dr \quad (53)$$

Inserting Eq. (49) into Eq. (53), it becomes

$$W_B=2M_P\int_r\frac{2\Delta z}{\eta_\rho}\sqrt{1-m\left(\frac{r-r_b}{r_c-r_b}\right)}\,dr \quad (54)$$

The total bending energy has the lowest value when $m_c=1$.

As a result of the above procedures, the working forces can be estimated.

The force acting on the roller can be resolved into F_f and F_n, to match the values of force measured by the tool dynamometer.

Then,

$$\begin{aligned}F_f&=-F_r\sin\alpha+F_z\cos\alpha\\F_n&=F_r\cos\alpha+F_z\sin\alpha\end{aligned} \quad (55)$$

3. Discussion

In this section, the working forces calculated by the present theory are compared with the theoretical and experimental values for 6 different working conditions in the Fig. 4. The comparative investigations are executed for the working forces of the present theory and experiment.

Figure 5 shows the effect of feed on the working forces, where it can be seen that, as the feed f increases, the working forces increase gradually. Namely, increasing the feed causes the rapid in-

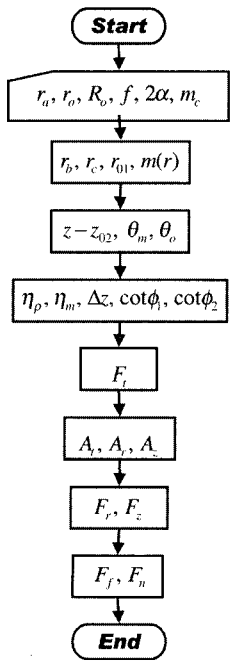

Fig. 4 The flow chart for calculating Forces

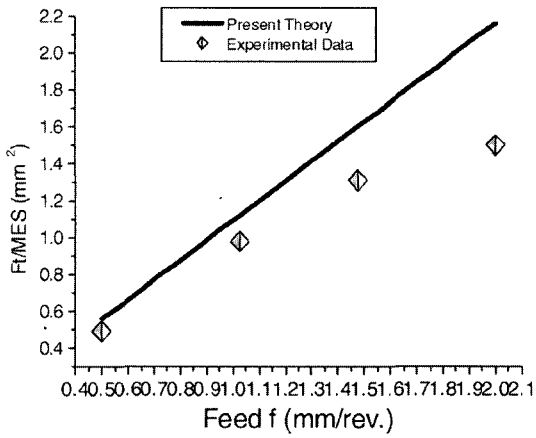

(a) Tangential force

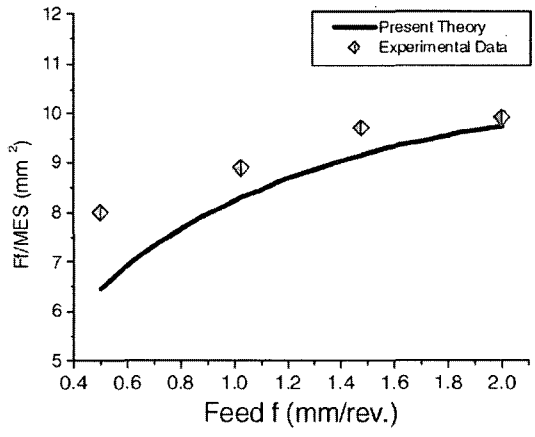

(b) Feed force

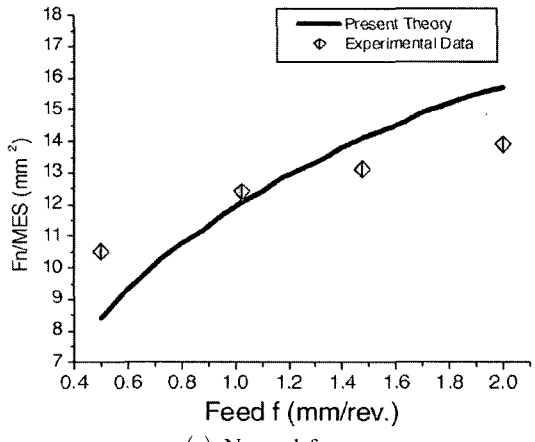

(c) Normal force

Fig. 5 Relation between Forces and Feed of Roller
f Working condition : Table 1-(a)

Table 1 Working Conditions in Shear Spinning of Cones

Condition	(a) Fig. 5	(b) Fig. 7	(c) Fig. 8	(d) Fig. 9	(e) Fig. 10	(f) Fig. 11
Half Cone Angle α (deg.)-ALPA	22.5°	22.5°	22.5°	22.5°	15.0~30.0°	30.0°
Diameter of Roller D_R (mm)	74	30~120	74	74	74	74
Round-off Radius r_o	4.0	4.0	2.0~12.0	4.0	4.0	4.0
Feed f (mm/rev.)	0.5~2.0	1.0	1.0	1.0	1.0	0.1~1.1
Thickness t_o (mm)	2.0	2.0	2.0	1.0~3.0	2.0	1.5
Measuring Radius r_a (mm)	40.0	40.0	40.0	40.0	40.0	34.0
Mean Flow Stress $\bar{\sigma}_m$ (kg/mm^2)	13.50	13.50	13.50	14.7~12.7	13.50	11.40
Young's Modulus E (kg/mm^2)	7200	7200	7200	7200	7200	7200
Revolution per Minutes N (rpm)	440	440	440	440	440	540

crease in tangential force. For small feed, the calculated tangential forces are in good agreement with experiments than for big feed. As the feed gets bigger the spinning process becomes unstable and shows the tendency of underspining, which gives lower tangential forces.

Figure 6 show the values of $\bar{\varepsilon}$ decrease as the feed gets bigger. For big feed of about 2 mm/rev., the value of $\bar{\varepsilon}$ is nearly equal to $(\cot\alpha)/\sqrt{3}$. This means that, for big feed and for strain-hardening material, the present solution can give lower working forces than the simple shear theory because of the different definition for $\bar{\sigma}_m$.

The effect of diameter of roller, D_R, on working forces is shown in Fig. 7. For bigger roller diameter, the theory gives good results. But for small diameter of roller, some difference is noticed. Small diameter of roller cannot be used in actual processes.

The effect of round-off of roller r_o on working forces are shown in Fig. 8. It can be seen that the working forces are not influenced nearly by the radius of round-off of roller, that is, as the radius of round-off of roller gets bigger, the working forces change slightly.

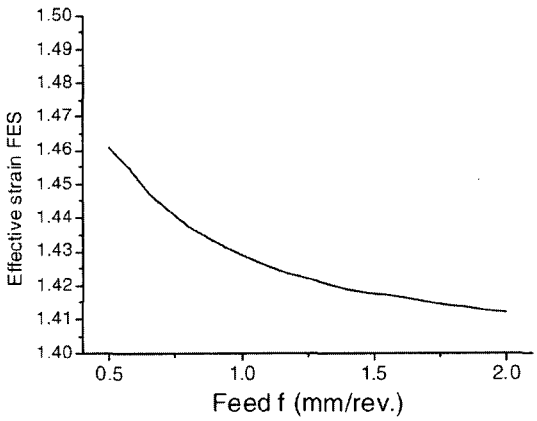

Fig. 6 Relation between Finite effective strain and Feed of Roller f Working condition : Table 1-(a)

The effect of blank thickness t_o on working forces is shown in Fig. 9. As the thickness of blank gets thicker, the working forces are increased, but the value of $\bar{\varepsilon}$ remains constant. Especially, the combination of some process variables, which contain large diameter of roller, large round-

off radius of roller, small feed and thick blank thickness, yield large differences on feed and normal forces.

The effect of cone angle of mandrel 2α on

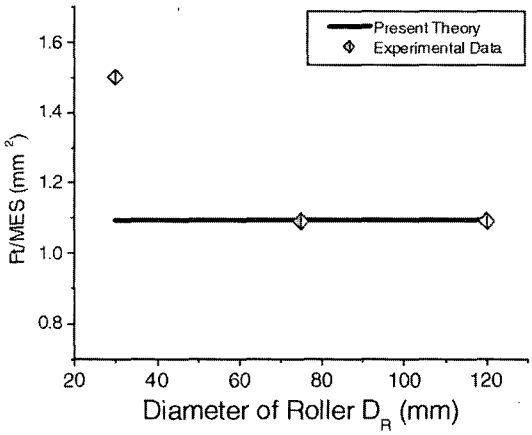

(a) Tangential force

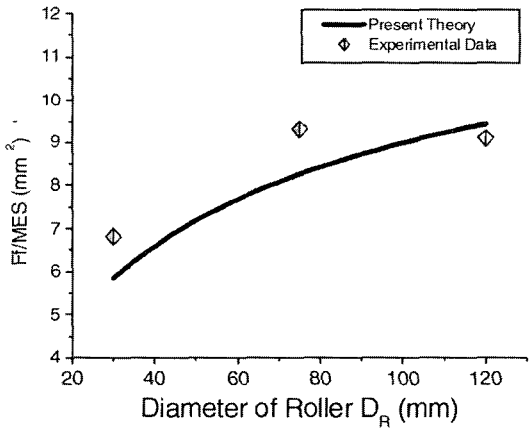

(b) Feed force

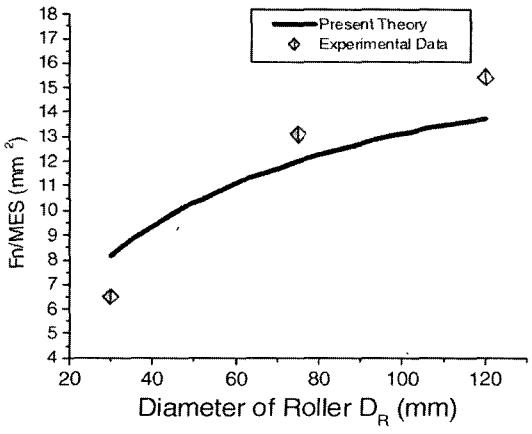

(c) Normal force

Fig. 7 Relation between Forces and Diameter of Roller Working D_R condition : Table 1-(b)

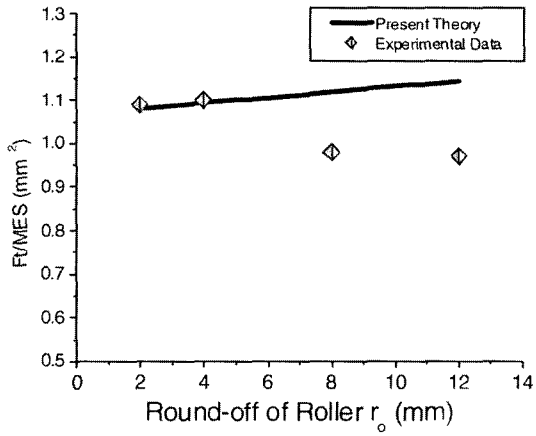

(a) Tangential force

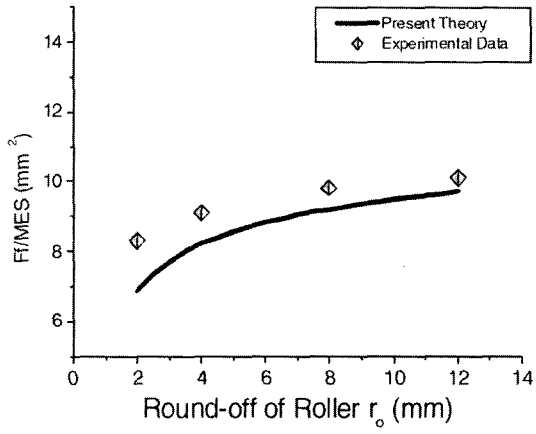

(b) Feed force

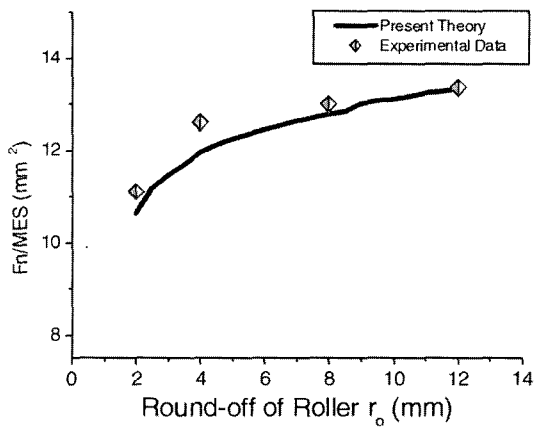

(c) Normal force

Fig. 8 Relation between Forces and Radius of Round-off of Roller r_o Working condition : Table 1-(c)

working forces is shown in Fig. 10, the working forces are on the decrease in its value, as the cone angle of mandrel gets bigger. But, for normal forces, the solid lines, show the opposite inclina-

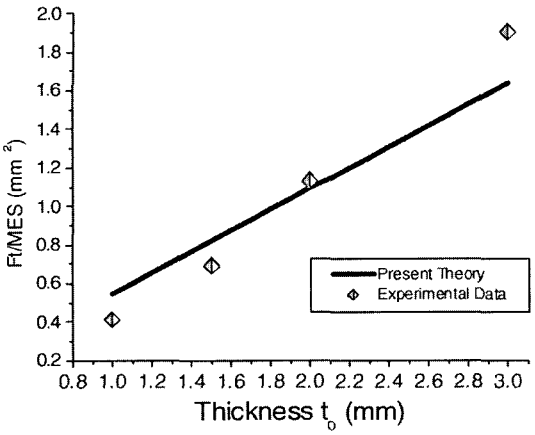

(a) Tangential force

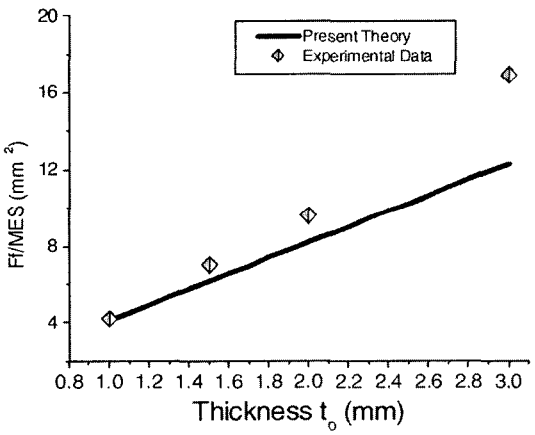

(b) Feed force

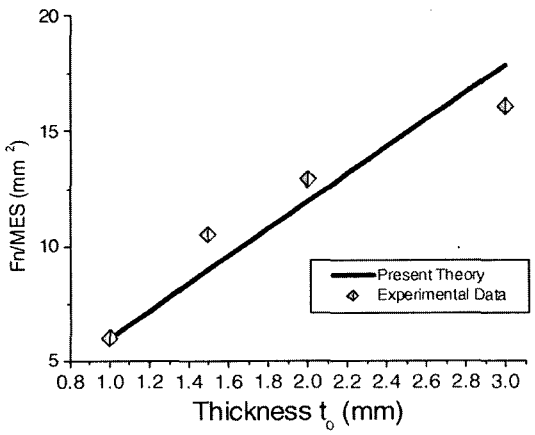

(c) Normal force

Fig. 9 Relation between Forces and Thickness of Blank Working t_o condition : Table 1-(d)

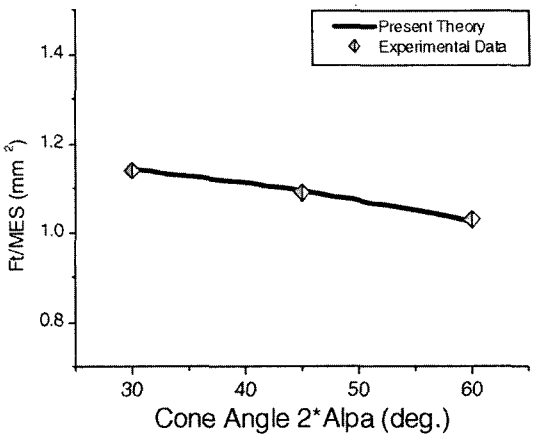

(a) Tangential force

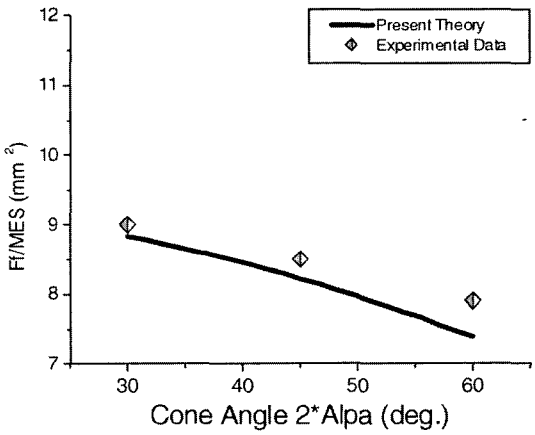

(b) Feed force

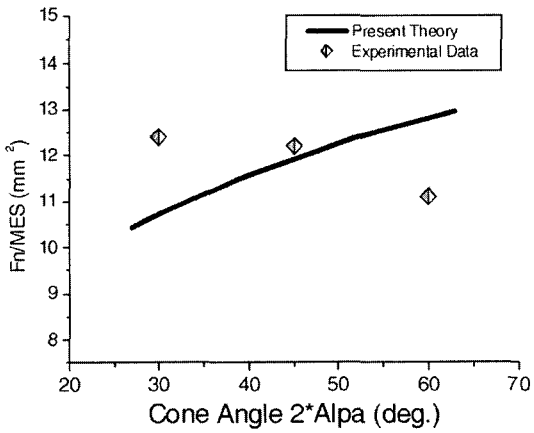

(c) Normal force

Fig. 10 Relation between Forces and Cone Angle of Mandrel Working 2α condition : Table 1-(e)

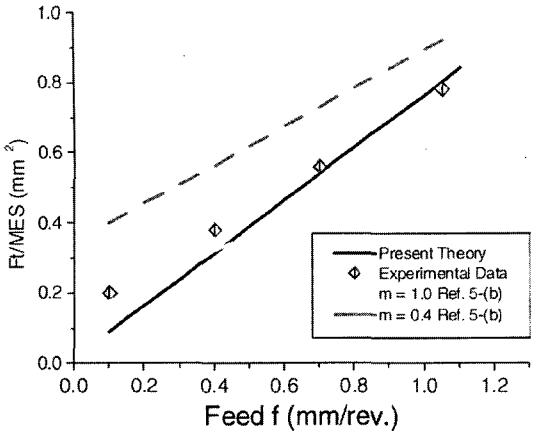

Fig. 11 Relation between Forces and Feed of Roller f in accordance with m Working condition : Table 1-(f)

tion. It can be seen that the theoretical values agree with the experimental ones for the working forces, that is, these phenomena do not affect the validity of the theory.

And Fig. 11 denotes the calculated and measured values for tangential force of Hayama et al. (1964), where M. Hayama et al. did not give any proper explanation of determinating the effective stress, $\bar{\sigma}_m$.

Their theoretical values for the proposed contact factor, m, are in accordance with the experimental values.

The tangential force in spinning is a very important quantity and is of great interest both to the designers of power spinning machines and to the production engineers faced with the problems of sufficient power to carry out the spinning operation. It is encourageous to note that these are reasonable agreements between the present theory and experimental results.

4. Conclusion

In the study of the mechanics of the shear spinning of cones, the following conclusions have been reached ;

(1) The theoretical equations for the tangential force component given by Eq. (39), which is based on the new deformation model, are good agreement with the experimental results.

(2) The normal and feed force components calculated from the relations of the theoretical contact areas show also reasonable agreement between theory and experiments, which indicate, in pact, that the ratios of the three forces are nearly equal to the ratios of the respective projected contact areas in three directions.

(3) From the deformation model proposed newly, the shear stress, τ_{rz} becomes k, yield limit in pure shear, in the deformation zone (Eq. (33)).

(4) The good theortical results can be obtained from the definition for the contact factor, $m(r)$, which is proposed as the Eq. (49).

References

Avitzur, B. and Yang, C. T., 1960, "Analysis of Power Spinning of Cones," *Journal of Engineering for Industry, TRANS. ASME, Series B*, Vol. 82, pp. 231~245.

Colding, B.N., 1959, "Shear Spinning," *ASME*, No. 59-prod-2.

Hayama, M. and Amano, T., 1975, "Analysis of Contact Form of Roller on Sheet Blank in Shear Spinning of Cones," *Journal of JSTP*, Vol. 16, No. 174.

Hayama, M. and Amano, T., 1975, "Experiments on the Mechanism of Shear Spinning of Cones," *Journal of JSTP*, Vol. 16, No. 172.

Hayama, M., 1975, "Analysis of Working Forces in Shear Spinning of Cones," *Journal of JSTP*, Vol. 16, No. 175.

Hayama, M., Murota, T. and Kudo, H., 1964, "Study of Shear Spinning,"

A) 1st Report, TRANS. JSME, Vol. 30, No. 220, 1964.

B) 2nd Report, TRANS. JSME, Vol. 30, No. 220, 1964.

C) 3rd Report, TRANS. JSME, Vol. 31, No. 228, 1965.

Kalpackcioglu, S., 1961, "On the Mechanics of Shear Spinning," *Journal of Engineering for Industry, TRANS. ASME, Series B*, Vol. 83, pp. 125~130.

Kegg, R. L., 1961, "A New Test Method for Determination of Spinnability of Metals," *Jour-*

nal of Engineering for Industry, TRANS. ASME, Series B, pp. 119~124.

Kobayashi, S., Hall, I. K. and Thomsen, E. G., 1961, "A Theory of Shear Spinning of Cones," *Journal of engineering for industry, TRANS. ASME, Series B*, Vol. 83, pp. 485~495.

Sortais, H. C., Kobayashi, S. and Thomsen, E. G., 1963, "Mechanics of Conventional Spinning," *Journal of Engineering for Industry, TRANS. ASME, Series B*, Vol. 85, pp. 44~48.